A Bottom-Up Demand-Side Energy System Model considering Dynamics of Heat Pump Water Heater and CO_2 Emission Factors

Tomohiro Katsuzaki[1], Ryuto Shigenobu[2],
Akiko Takahashi[3], Masakazu Ito[2], Yosuke Suzuki[3], Hiroaki Terasaki[2]

[1]Advanced Interdisciplinary Science and Technology, Graduate School of Engineering, University of Fukui, Fukui, Japan
[2]Faculty of Engineering, University of Fukui, Fukui, Japan
[3]Headquarters for Carbon Neutral Initiatives, Faculty of Basic and Generic Researches, University of Fukui, Fukui, Japan

Abstract - Promoting green transformation (GX) is imperative for Japan's carbon neutrality. This paper focuses on a demand-side energy system (DES) for a household, optimizing technology selection and operation scheduling to minimize CO_2 emissions. We have slightly modified the CO_2 emission calculation in our previous model, originally incorporating the dynamic behavior of a heat pump water heater (HPWH), to analyze the impact of the dynamic CO_2 emission factors on technology selection and operation scheduling. Simulation results indicate that incorporating the dynamic factors increases the capacity of a battery electric vehicle (BEV) charger and confirms time shifts in electricity usage by the BEV as well as self-consumption patterns of the HPWH. Future research will extend simulation periods, explore diverse seasonal and regional scenarios, and incorporate planning strategies to support Japan's GX initiatives further.

Keywords: technology selection, capacity planning, operation scheduling, household, energy management system, mixed-integer linear programming

1. Introduction

Green transformation (GX), which accelerates the integration of renewable energy (RE) and reduces dependence on fossil fuels, is a critical initiative in Japan, propelling the nation toward carbon neutrality [1]. In the fiscal year 2022, the commercial and residential sectors combined accounted for approximately 31.2% of Japan's total final energy consumption [2], underscoring the urgent need for effective GX strategies in these domains.

In this study, we focus on a demand-side energy system (DES) for an individual household, investigating both optimal technology selection and operation scheduling to minimize total CO_2 emissions. In our previous research, we developed a bottom-up energy system model that can analyze time variations in the coefficients of performance (COPs) by considering the dynamic behavior of a heat pump water heater (HPWH) [3]. Our previous research assumed that surplus power generated by a rooftop photovoltaic (PV) system could invariably be sold back to the grid, resulting in significant CO_2 emission reductions [3]. However, in practice, the ability to sell surplus PV power is contingent upon utility operating conditions and the area's electricity energy mix. During periods when the grid relies predominantly on fossil fuels or encounters renewable integration constraints, utilities may impose output control commands that limit the amount of power returned to the grid [4]. Consequently, a planner such as a DES designer must account for time-varying grid conditions when making decisions regarding both technology selection and operation scheduling.

To address these challenges, our current research introduces dynamic CO_2 emission factors that reflect the utility's energy mix at different times [5]. These factors capture variations in power supply composition, specifically, the proportions of thermal and renewable generation, thus enabling more informed decision-making concerning the selection of technologies, such as the HPWH, a gas water heater (GWH), and the rooftop PV system, as well as their operation. By integrating the dynamic factors into the optimization model, our approach aims to guide DES planning toward achieving lower life-cycle CO_2 emissions and to analyze its impact on the DES planning. Accordingly, this paper discusses the differences in optimization results between static and dynamic CO_2 emission factors for a household in Fukui, Japan, over a five-day winter period.

2. Mathematical model

In this study, the mixed-integer linear programming (MILP) model "JOP-TSCPOS-DES" from Reference [3] is modified. This paper describes only assumed DES and important/modified points of the JOP-TSCPOS-DES.

2.1 Assumed demand-side energy system

The technologies (equipment types) that are candidates for introduction into the DES are a PV array (PVA), a hybrid power conditioner (HPC), a battery (BAT), a BAT charger/discharger (BCD), a battery electric vehicle (BEV), a BEV charger/discharger (VCD), a power switching unit (PSU), a smart distribution board (SDB), a gas water heater (GWH), a hot water tank (HWT), a solar thermal collector (STC), a heat pump unit (HPU), and a gasoline engine vehicle (GEV). As loads of the DES, an alternating current electrical power load (AEL), a hot water load (HWL), a tap water cold water load (CWL), a running electrical power load for BEV (REL), a running gasoline load for GEV (RGL) are considered. The assumed configuration of the DES for a household [3] is shown in Figure 1. For simplicity of the model, it is assumed that the HWT is always technology-selected (introduced as a ready-made (RM) capacity).

2.2 Dynamics of heat pump water heater

In the JOP-TSCPOS-DES, the dynamics of the HPWH are considered as time-varying of stored hot water temperatures, stored hot water volumes, stored thermal energies, target heating temperatures, COPs, input electrical powers, and output thermal powers are considered, respectively.

The dynamic relationships between COPs, input electrical powers, and output thermal powers are expressed as follows:

$$r^{\mathrm{COP,heat}}_{\mathrm{HPU},k} = \hat{\eta}_{\mathrm{HPU},k}\left(\alpha^{\mathrm{heat}}_{\mathrm{HPU}} + \beta^{\mathrm{heat}}_{\mathrm{HPU}}\hat{T}_k - \gamma^{\mathrm{heat}}_{\mathrm{HPU}} T_{\mathrm{HWT},k} - \delta^{\mathrm{heat}}_{\mathrm{HPU}} T^{\mathrm{heat}}_{\mathrm{HPU},k+1}\right),\ \forall k \in \mathcal{K}, \quad (1)$$

$$P^{\mathrm{heat}}_{\mathrm{HPU},k} = W^{\mathrm{heat}}_{\mathrm{HPU},k} / r^{\mathrm{COP,heat}}_{\mathrm{HPU},k},\ \forall k \in \mathcal{K}, \quad (2)$$

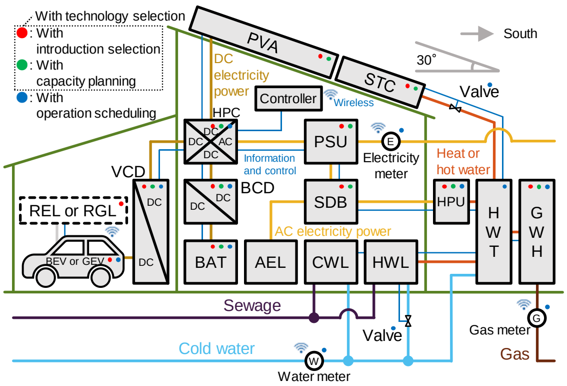

Figure 1 Assumed configuration of demand-side energy system for household [3]

where

$$\hat{\eta}_{\mathrm{HPU},k} \triangleq \begin{cases} \eta_{\mathrm{HPU}} & \text{if } \hat{T}_k \le T^{\mathrm{DTH}} \\ 1 & \text{otherwise} \end{cases},\ \forall k \in \mathcal{K}, \quad (3)$$

$$r^{\mathrm{COP,heat,on}}_{\mathrm{HPU},k} \triangleq \begin{cases} r^{\mathrm{COP,heat}}_{\mathrm{HPU},k} & \text{if } 0 < P^{\mathrm{heat}}_{\mathrm{HPU},k} \\ 0 & \text{otherwise} \end{cases},\ \forall k \in \mathcal{K}, \quad (4)$$

with k is a time section number, $\mathcal{K} \triangleq \{1,2,\cdots\}$ is a finite set of k, $\hat{\eta}_{\mathrm{HPU},k}$ is a predicted coefficient of the HPU at k indicating whether there is a reduction in efficiency due to a defrosting operation, $\alpha^{\mathrm{heat}}_{\mathrm{HPU}}$, $\beta^{\mathrm{heat}}_{\mathrm{HPU}}$, $\gamma^{\mathrm{heat}}_{\mathrm{HPU}}$, and $\delta^{\mathrm{heat}}_{\mathrm{HPU}}$ are regression coefficients for the calculation of the COP of the HPU, $\hat{T}_k$ is a predicted outdoor temperature at k, $T_{\mathrm{HWT},k}$ is the stored water temperature of the HWT at k, $T^{\mathrm{heat}}_{\mathrm{HPU},k}$ is a potential of the target heating temperature of the HPU at k, $r^{\mathrm{COP,heat}}_{\mathrm{HPU},k}$ is a potential of the COP of the HPU at k, $W^{\mathrm{heat}}_{\mathrm{HPU},k}$ is the output thermal power of the HPU at k, $P^{\mathrm{heat}}_{\mathrm{HPU},k}$ is the input electrical power of the HPU at k, η_{HPU} is the efficiency of the HPU at the defrosting operation, T^{DTH} is a threshold value of the outside temperature for switching between a normal operation and the defrosting operation of the HPU, named as a defrosting threshold (DTH) temperature, $r^{\mathrm{COP,heat,on}}_{\mathrm{HPU},k}$ is the COP of the HPU at k.

2.3 Dynamics of CO_2 emission factors

The dynamic CO_2 factors are estimated by method A in Reference [5]. The estimated factors exhibited high values when thermal power generation is high in the area's energy mix and low when PV output is high. In this context, the DES is expected to plan its operation schedules such that surplus PV power is sold when the CO_2 factor is high and grid power is purchased when the factor is low, thereby reducing overall CO_2 emissions. In other words, it is anticipated that the technology selection and operation scheduling of the DES using the factors will render it less likely to issue output control commands.

2.4 Modified part of optimization model

The Static CO_2 emissions formula expressed as Equation (106) in Reference [3] for the

JOP-TSCPOS-DES can be replaced by the dynamic CO_2 emissions formulas as follows:

$$\begin{bmatrix} G^{\mathrm{ele,buy,PR}} \\ G^{\mathrm{ele,sell,PR}} \end{bmatrix} \triangleq \begin{bmatrix} \sum_{k\in\mathcal{K}}\left(\hat{g}_k^{\mathrm{ele}} P_{\mathrm{ESM},k}^{\mathrm{buy}} \Delta k\right) \\ \sum_{k\in\mathcal{K}}\left(\hat{g}_k^{\mathrm{ele}} P_{\mathrm{ESM},k}^{\mathrm{sell}} \Delta k\right) \end{bmatrix}, \tag{5}$$

where Δk is a granularity of the time section, $\hat{g}_k^{\mathrm{ele}}$ is the predicted dynamic CO_2 emission factor of the electric utility at k, $P_{\mathrm{ESM},k}^{\mathrm{buy}}$ and $P_{\mathrm{ESM},k}^{\mathrm{sell}}$ are buying and selling power measured by the ESM at k (buying power from and selling power to the utility by the DES consumer), respectively, $G^{\mathrm{ele,buy,PR}}$ and $G^{\mathrm{ele,sell,PR}}$ are the pro-rated (PR) total CO_2 emissions and emission reductions from buying and selling power, respectively.

3. Case study

This paper analyzes the impact of changing the CO_2 emission factors from static to dynamic on both optimal technology selection and operation scheduling, using the instance of Case 2by in Reference [3].

3.1 Simulation conditions

The objective in Case 2by is to find technology selection and operation schedules that minimize the life cycle CO_2 emissions for a four-person household in Fukui, Japan. Important conditions are the planning period $\mathcal{K}$ is 5 days (Δk is 1 hour, mixed sunny, cloudy, and rainy days in December of winter when both electricity and hot water demands are high and the required capacities of various equipment are expected to be maximized), PVA and STC are only installed on the roof (maximum installation area is 80 m^2), and there are no output control commands for surplus power sales (power can be sold up to the lead-in wire capacity of 6 kW).

The setting of the static and dynamic CO_2 emission factors for this case study are shown in Figure 2 (a). The dynamic factors were estimated using Hokuriku Electric Power Transmission & Distribution Company's actual area supply and demand [6] for the fiscal year 2023, and the values of the dynamic factors are adjusted so that the average values of the dynamic and static factors match Hokuriku Electric Power Company's adjusted average CO_2 emission factor [7] for the fiscal year 2023.

3.2 Simulation results

Table 1 shows the comparison of computed technology selection (introduction selection and capacity planning for the equipment) for the DES under the different CO_2 emission factors. As shown in Table 1, although the equipment introduction selection remained unchanged between the static and dynamic cases, it can be observed that in the dynamic case, the capacity of the VCD

Table 1 Comparison of computed technology selection (introduction selection and capacity planning for equipment) for demand-side energy system under different CO_2 emission factors

Factor types	Equipment capacity types							
	C_{PVA}^{*} [kW]	C_{HPC}^{*} [kW]	C_{BCD}^{*} [kW]	C_{VCD}^{*} [kW]	C_{BAT}^{*} [kWh]	C_{BEV}^{*} [kWh]	C_{PSU}^{*} [kW]	C_{SDB}^{*} [kW]
Static	15.9	9.4	-	1.4	-	35.8	9.4	3.5
Dynamic	15.9	9.2	-	2.6	-	35.8	9.2	3.2
Increase	0.0%	-2.1%	-	85.7%	-	0.0%	-2.1%	-8.6%
Select	$\checkmark^{*}$	$\checkmark^{*}$	$\times^{*}$	$\checkmark^{*}$	$\times^{*}$	$\checkmark^{\mathrm{RM},*}$	$\checkmark^{*}$	$\checkmark^{*}$
Factor types	**Equipment capacity types**							
	C_{GWH}^{*} [kW]	C_{HWT} [kWh]	$V_{\mathrm{HWT}}^{\mathrm{cap}}$ [L]	N_{STC}^{*} [item]	$C_{\mathrm{HPU}}^{\mathrm{heat},*}$ [kW]	C_{GEV}^{*} [L]	C_{ESM}^{*} [kW]	$C_{\mathrm{ESM}}^{\mathrm{use},*}$ [kW]
Static	15.0	41.6	370	-	11.7	-	6.0	6.0
Dynamic	15.0	41.6	370	-	11.0	-	6.0	6.0
Increase	0.0%	0.0%	0.0%	-	-6.0%	-	0.0%	0.0%
Select	$\checkmark^{*}$	$\checkmark^{\mathrm{RM}}$	$\checkmark^{\mathrm{RM}}$	$\times^{*}$	$\checkmark^{*}$	$\times^{\mathrm{RM},*}$	$\checkmark^{*}$	$\checkmark^{*}$

Here, $C_e^{*},\ \forall e \in \{\mathrm{PVA, HPC, BCD, VCD, BAT, BEV, PSU, SDB, GWH, GEV}\}$ and $C_{\mathrm{HPU}}^{\mathrm{heat},*}$ are the computed capacity of e and the HPU, respectively, N_{STC}^{*} is the computed number of panels of the STC, C_{HWT} and $V_{\mathrm{HWT}}^{\mathrm{cap}}$ are the set capacity of the HWT in energy and volume, respectively, C_{ESM}^{*} and $C_{\mathrm{ESM}}^{\mathrm{use},*}$ are the computed contracted power for and maximum utilization capacity of the ESM, respectively, $\checkmark^{*}$ and $\times^{*}$ are the computed selection of introduction and non-introduction of the equipment, respectively, $\checkmark^{\mathrm{RM},*}$ and $\checkmark^{\mathrm{RM}}$ are the computed and set selection of introduction and non-introduction of the equipment with RM capacity, respectively, where e is an index variable.

Table 2 Comparison of computed 5-day pro-rated costs and CO_2 emissions for demand-side energy system under different CO_2 emission factors

Factor types	Cost types [JPY]					
	$Y^{\mathrm{ele,PR},*}$	$Y^{\mathrm{gas,PR},*}$	$Y^{\mathrm{water,PR},*}$	$Y^{\mathrm{oil},*}$	$Y^{\mathrm{ini,DC},*}$	$Y^{\mathrm{total,PR},*}$
Static	4,873	1,304	1,289	0	20,951	28,416
Dynamic	4,828	1,208	1,289	0	21,212	28,536
Increase	-0.9%	-7.4%	0.0%	-	1.2%	0.4%
Factor types	**CO_2 emission types [kg-CO_2]**					
	$G^{\mathrm{ele,PR},*}$	$G^{\mathrm{gas,PR},*}$	$G^{\mathrm{water,PR},*}$	$G^{\mathrm{oil},*}$	$G^{\mathrm{ini,DC},*}$	$G^{\mathrm{total,PR},*}$
Static	40.15	10.55	2.21	0.00	39.97	92.86
Dynamic	44.92	9.69	2.21	0.00	40.20	97.00
Increase	11.9%	-8.2%	0.0%	-	0.6%	4.5%

Here, $Y^{x,\mathrm{PR},*}$ and $G^{x,\mathrm{PR},*}$ are the computed PR cost and CO_2 emissions of x, respectively, $Y^{\mathrm{oil},*}$ and $G^{\mathrm{oil},*}$ are the computed gasoline cost and CO_2 emissions of the GEV, respectively, $Y^{\mathrm{ini,DC},*}$ and $G^{\mathrm{ini,DC},*}$ are the computed depreciation (DC) cost and CO_2 emissions of equipment, respectively, $\forall x \in \{\mathrm{ele, gas, water, total}\}$, where x is an index variable, ele is an abbreviation of electricity.

increased by 85.7%, while the capacity of the HPU decreased by 6.0% compared to the static case. This suggests that the dynamic CO_2 emission factors, which reflect the thermal power generation ratio of the utility, have the potential to modify the capacity of certain energy storage systems, yet may not be sufficient to alter the equipment introduction selection. Moreover, to induce changes in the equipment introduction selection, it may be preferable to utilize dynamic electricity rates that are subject to manual adjustments by electric utilities or similar entities.

Table 2 shows the comparison of computed 5-day pro-rated costs and CO_2 emissions for the DES under different CO_2 emission factors. From Table 2, it is confirmed that both the total cost and the total CO_2 emissions remain nearly unchanged.

In particular, in the dynamic case compared to the static case, the gas cost and gas CO_2 emissions decreased by 7.4% and 8.2%, respectively, which indicates an improvement in the electrification rate of the supply energy used to meet hot water demand. On the other hand, while the CO_2 emissions from electricity increased by 11.9%, the depreciation-related CO_2 emissions of the equipment showed almost no increase. This suggests that the increase in the depreciation CO_2 emissions due to the introduction of new equipment outweighs the CO_2 reduction achieved by operating. In other words, insufficient equipment has been introduced to fully realize the benefits of dynamic factor's operation.

Figure 2 also presents the comparison of computed 5-day supply and demand schedules for the demand-side energy system under different CO_2 emission factors. In Figure 2, the BEV charging times are depicted by horizontal bar graphs, and it can be observed that in the dynamic case, the charging periods during the low CO_2 emission factor hours have shifted relative to the static case. This indicates that operation schedules aligned with the dynamic CO_2 emission factors were implemented. Furthermore, in Figure 2 (c) for the dynamic case, on sunny days (Day 1 and Day 3) there are periods during which surplus power from the PVA is used as the input power for the HPU that is, renewable energy self-consumption is observed. However, since the majority of the surplus PV power is used for grid sales, even with the dynamic factors considered, the suppression of reverse power flow was not achieved. This is likely because power sales are assumed to yield a CO_2 reduction effect equivalent to the emission factor maintained by the utility. Moreover, grid sales, which are not affected by conversion efficiency losses, are prioritized over self-consumption, where such losses reduce the CO_2 reduction benefit.

In any case, even with the simultaneous optimization of technology selection and operation scheduling aimed at minimizing CO_2 emissions by incorporating dynamic factors for current RE equipment, the reduction of output control commands may not be achieved. This suggests that further technological innovations, such as cost minimization incorporating dynamic electricity rates and efficiency improvements in existing RE equipment, may be necessary to reduce output control commands.

Figure 3 presents the comparison of computed 5-day total output thermal energy and the variations in the outputs/COPs of the HPU for the DES under different CO_2 emission factors. From the left panel of Figure 3, it can be observed that the electrification rate increased by 3.1 percentage points in the dynamic case compared to the static case.

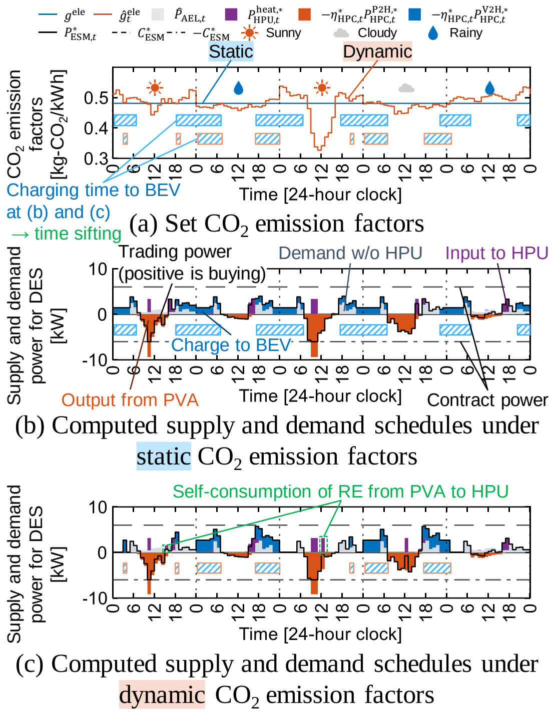

(a) Set CO_2 emission factors

(b) Computed supply and demand schedules under static CO_2 emission factors

(c) Computed supply and demand schedules under dynamic CO_2 emission factors

Here, g^{ele} and $\hat{g}_t^{\mathrm{ele}}$ are the set static and dynamic CO_2 emission factor at t, respectively, $\hat{P}_{\mathrm{AEL},t}$ is a set predicted demand power of the AEL at t, $P_{\mathrm{HPU},t}^{\mathrm{heat},*}$ is the computed input power of the HPU at t, $\eta_{\mathrm{HPC},t}^{*}$, $P_{\mathrm{HPC},t}^{\mathrm{P2H},*}$, and $P_{\mathrm{HPC},t}^{\mathrm{V2H},*}$ are computed conversion efficiency, output power from the PVA to the PSU, and charging/discharging power from the VCD to the PSU (positive is discharging to the PSU) of the HPC at t, respectively, $P_{\mathrm{ESM},t}^{*}$ is a computed trading power measured by the ESM at t (positive is buying power from the utility by the DES consumer), where t is an index variable for continuous time.

Figure 2 Comparison of computed 5-day supply and demand schedules for demand-side energy system under different CO_2 emission factors

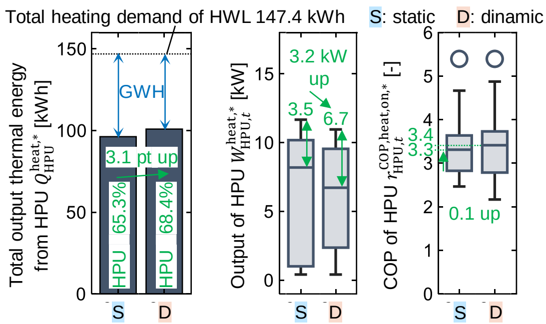

Figure 3 Comparison of computed 5-day total output thermal energy and variations in outputs/coefficients-of-performance of heat pump unit for demand-side energy system under different CO_2 emission factors

Meanwhile, from the central panel, it is confirmed that in the dynamic case, the difference between the maximum (equal to the capacity) and median output power of the HPU increased by 3.2 kW relative to the static case. This indicates that the HPU tends to operate under lower load conditions in the dynamic case, underscoring the importance of considering dynamics [3]. Additionally, from the right panel, the median COP of the HPU increased by 0.1 in the dynamic case compared to the static case, indicating improved operational efficiency of the HPU. In summary, adopting the more realistic dynamic emission factors instead of the static ones not only emphasizes the importance of accounting for dynamics but also suggests that the previously underestimated benefits of improved electrification and efficiency of the HPWH can be appropriately assessed.

4. Conclusion

This study investigated the impact of incorporating dynamic CO_2 emission factors into the bottom-up DES model for a household. Simulation results indicate that while the overall equipment introduction selection remains unchanged between the static and dynamic cases, the capacity planning is significantly affected. In particular, the capacity of the VCD increased by 85.7%, and the capacity of the HPU decreased by 6.0% under the dynamic CO_2 emission factors. These findings suggest that dynamic factors, which more accurately reflect the utility's time-varying energy mix, can influence specific aspects of the DES design, especially in terms of storage system capacities, without necessarily altering the initial equipment selection.

Furthermore, the analysis reveals that dynamic CO_2 emission factors lead to noticeable shifts in operation schedules, such as modified BEV charging times and improved operational efficiency of the HPWH (as evidenced by an increased median COP and higher electrification rates). However, the overall system cost and total CO_2 emissions remain nearly unchanged, implying that the current level of equipment adoption may not be sufficient to fully harness the benefits of dynamic operation. This underscores the potential need for complementary strategies, such as dynamic electricity rates, to further optimize DES performance and reduce output control commands.

Future work will extend simulation periods, explore diverse seasonal and regional scenarios, and integrate advanced planning strategies to enhance the DES design, thereby supporting Japan's green transformation initiatives more effectively.

Acknowledgments

This work was supported by JST Grant Number JPMJPF2012 and the Graduate Program for Power Energy Professionals, Waseda University from MEXT WISE Program.

References

[1] "The Basic Policy for the Realization of GX," METI, Tokyo, Japan, Feb. 10, 2023. [Online]. Available: https://www.meti.go.jp/english/press/2023/pdf/0210_003a-2.pdf

[2] "FY2022 Energy Supply and Demand Report (Revised Report)" [in Japanese], ANRE, METI, Tokyo, Japan, Apr. 12, 2024. [Online]. Available: https://www.enecho.meti.go.jp/statistics/total_energy/pdf/honbun2022fykaku.pdf

[3] T. Katsuzaki et al., "Optimal Joint Planning of Technology Selection, Capacities Planning, and Operation Scheduling for Demand-Side Energy System considering Dynamics of Heat Pump Water Heater and Linkage of Electricity, Heat, and Water" [Preprint] [in Japanese], *Jxiv*, Version 3, Mar. 5, 2025, doi: 10.51094/jxiv.1066.

[4] "Short-Term Outlook for Renewable Energy Output Control" [in Japanese], ANRE, METI, Tokyo, Japan, Jan. 23, 2025. [Online]. Available: https://www.meti.go.jp/shingikai/enecho/denryoku_gas/saisei_kano/smart_power_grid_wg/pdf/001_02_01.pdf

[5] X. Shi et al., "Estimation of Hourly CO_2 Emission Factor by General Power Transmission Companies" [in Japanese], in *Online Tech. Papers of Annu. Meeting SHASEJ*, 2020, vol. 10, pp. 449–452, doi: 10.18948/shasetaikai.2020.10.0_449.

[6] Hokuriku Electric Power Transmission & Distribution Company, "Energy Supply and Demand Data (Download)" [in Japanese], Hokuriku Electric Power Transmission & Distribution Company Website. Accessed: Mar. 18, 2025. [Online]. Available: https://www.rikuden.co.jp/nw_jyukyudata/area_jisseki.html

[7] Hokuriku Electric Power Company, "Trends in CO_2 Emission Factors and Emissions on Electric Utility" [in Japanese], Hokuriku Electric Power Company Website. Accessed: Mar. 19, 2025. [Online]. Available: https://www.rikuden.co.jp/onshitsukoka/

Corresponding author

Tomohiro Katsuzaki
E-mail: katsuzaki.tomohiro@pws.fuee.u-fukui.ac.jp